Protein Engineering

Deutsche Ausgabe: DOI: 10.1002/ange.201507094
Internationale Ausgabe: DOI: 10.1002/anie.201507094

Designing Light-Activated Charge-Separating Proteins with a Naphthoquinone Amino Acid

*Bruce R. Lichtenstein, Chris Bialas, José F. Cerda, Bryan A. Fry, P. Leslie Dutton, and Christopher C. Moser**

Abstract: *The first principles design of manmade redox-protein maquettes is used to clarify the physical/chemical engineering supporting the mechanisms of natural enzymes with a view to recapitulate and surpass natural performance. Herein, we use intein-based protein semisynthesis to pair a synthetic naphthoquinone amino acid (Naq) with histidine-ligated photoactive metal–tetrapyrrole cofactors, creating a 100 μs photochemical charge separation unit akin to photosynthetic reaction centers. By using propargyl groups to protect the redox-active para-quinone during synthesis and assembly while permitting selective activation, we gain the ability to employ the quinone amino acid redox cofactor with the full set of natural amino acids in protein design. Direct anchoring of quinone to the protein backbone permits secure and adaptable control of intraprotein electron-tunneling distances and rates.*

Protein semisynthesis is a powerful method for unraveling the physical/chemical engineering of natural enzyme mechanisms through the introduction of post-translational modifications, biophysical probes, or unnatural amino acids into proteins of any size.[1–4] As one example, semisynthetic intein chemistry was used to insert fluorinated tyrosines with altered phenolic pK_a values, but not altered redox potentials, to resolve the role of proton transfer in intraprotein radical electron transfer catalysis in ribonucleotide reductase.[5] Some of the most fundamental questions of natural-redox-protein engineering involve the physical/chemical interplay between redox cofactors and their protein environment.[6–9] Site-directed mutagenesis around cofactors and reconstitution with exotic cofactors are also important methods to clarify electron-transfer engineering.[10–13] However, as products of unplanned natural selection, native protein sequences tend to accumulate obscure and often unresolvable interdependencies between amino acids themselves and between amino acids and cofactors. As an alternative, we construct a wide range of artificial redox proteins that have minimal reference to any specific natural protein sequence and instead include simplified, first-principles-directed protein folding and reduced amino acid diversity.[14–16] These provide a platform to clarify the typical properties of redox cofactors in an unselected protein environment, identify what elements of protein engineering are effective in controlling the activity of redox cofactors in proteins, and resolve the roles of individual amino acids.

Our work on securing redox-active tetrapyrrole cofactors, such as hemes, chlorins, and bilins, and FeS clusters in the architecturally adaptable synthetic protein scaffolds known as maquettes,[14,17] exploits ligating His and Cys residues in the same way that these cofactors are covalently ligated in natural proteins. In contrast, the pivotal quinone cofactors used in respiration and photosynthesis to couple proton and electron transfer are frequently noncovalently and reversibly bound to natural protein sites. However, when quinones are mobile, it is less clear how modulation of the protein environment controls quinone chemical function. Secure cofactor positioning is also important to set desired intraprotein electron-tunneling rates, which change by an order of magnitude with every 1.7 Å change in cofactor separation.[18,19] Although quinones have been covalently attached to Cys residues,[20–23] accurate cofactor placement suffers from the relatively long and flexible thioether linkage. As described herein, we establish conformational confinement by creating a chemically protected unnatural quinone amino acid (Naq).[16,24] Solid-phase peptide synthesis is used to install this cofactor in an appropriate helical protein fragment. Intein-mediated protein semisynthesis is then exploited to place the quinone amino acid in a larger expressed protein environment near enough to other cofactors to participate in light-activated intraprotein electron-transfer reactions.

In maquette protein scaffolds, Gly-rich loop sequences connect extended runs of amino acids with high alpha helix propensity that are arranged in a binary pattern such that one face of the helix is predominantly polar (Glu, Asp, Lys, or Gln) and the other nonpolar (Ala, Leu, Phe or Trp). In aqueous solution, burial of nonpolar faces drives assembly into a 4-helix bundle.[25] In principle there are two possible helix–loop topologies for bundle assembly, with the second helix assembling either clockwise relative to the first helix when viewed from the amino terminal (as shown in Figure 1) or counterclockwise (see Figure S5 in the Supporting Information). In either case, buried histidines are aligned to encourage axial bis-His ligation to both faces of a heme iron

[*] Dr. B. R. Lichtenstein,[+] C. Bialas,[+] B. A. Fry, Prof.Dr. P. L. Dutton, Dr. C. C. Moser
The Johnson Research Foundation
Department of Biochemistry and Biophysics
University of Pennsylvania, Philadelphia, PA 19104-6059 (USA)
E-mail: moserc@mail.med.upenn.edu
Dr. B. R. Lichtenstein[+]
Present address: Max Planck Institute for Developmental Biology
Tübingen, 72076 (Germany)
Dr. J. F. Cerda
Department of Chemistry, St. Joseph's University
Philadelphia, PA 19131 (USA)
[+] These authors contributed equally to this work.

Supporting information (including the Experimental Section) and ORCID(s) from the author(s) for this article are available on the WWW under http://dx.doi.org/10.1002/anie.201507094.

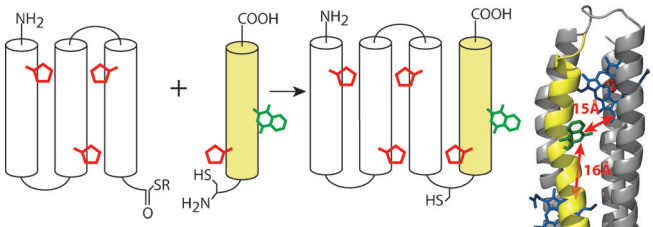

Helix : EIWKQHEDALQKFEE(E/Naq)ALNQFEDLKQL
Loop 1 and 2: GGSGSGSGG; Loop 3: GGSGCGSGG

Figure 1. The semisynthetic four α-helix maquette is constructed from the thioester of an expressed three-helix fragment and a synthetic helix with an N-terminal cysteine and an incorporated Naq residue. Expressed and synthetic helices are shown as gray and yellow cylinders, with tetrapyrrole-ligating histidine residues in red and synthetic naphthoquinone amino acid (Naq) residues in green, connected by glycine-rich loops shown as black arcs. The helices have nearly identical sequences (bottom), with a glutamate replaced by Naq in the fourth helix of the semisynthetic bundle. A molecular dynamics simulation structure (right) with Naq and two histidine-ligated tetrapyrroles (blue) places Naq nearly equidistant from both tetrapyrrole binding sites.

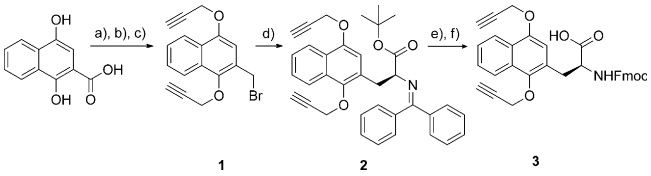

Scheme 1. Propargyl protected Fmoc-Naq synthesis. Conditions: a) Propargyl bromide, K_2CO_3, KI, DMF, 90 °C, 79 %; b) $LiAlH_4$, tetrahydrofuran, 0 °C to RT, 90 %; c) PBr_3, CCl_4, 0 °C, 92 %; d) diphenylmethylene glycine *tert*-butyl ether, $CsOH{\cdot}H_2O$, phase-transfer catalyst, toluene, −42 °C, 84 %, 96.5 % *ee*; e) ethanedithiol, TFA, 91 %; f) Fmoc-succinimide, $NaHCO_3$, DMF, 60 °C, quantitative.

or single His ligation of light-active Zn tetrapyrroles. By replacing a surface-exposed glutamic acid in the middle of the fourth helix with Naq, the environment around the amino acid is expected to vary little between the two topologies and the edge-to-edge distances between Naq and the bound metal–tetrapyrrole cofactors are similar (estimated from the model structure to be 14–16 Å, depending on the Naq rotamer).

The thioester-terminated fragment for protein semisynthesis (Figure 1) was derived from a previously described single chain multi-tetrapyrrole binding maquette sequence[15] by cloning the N-terminal three-helix fragment into the commercially available vector for intein-mediated protein (pKYB1; New England Biolabs). We avoided insolubility during expression by exchanging the provided intein fusion (Sce VMA intein fused with a chitin binding domain) with an alternative intein fusion (Mxe GyrA intein fused with a C-terminal hexahistidine affinity-tagged maltose binding protein).

For Naq to be activated in maquettes with unprotected generic side-chain functionalities, a new protecting group strategy was developed to avoid interference of Cys and Trp residues with the reported oxidative deprotection of Naq.[16] Although uncommon in peptide work, propargyl groups can be removed under a range of conditions, in solvents like trifluoroacetic acid (TFA) and dimethylformamide (DMF), compatible with longer peptides and proteins,[26–28] and their installation could be effected under similar conditions to the methyl groups of the original synthesis.

The synthesis of the propargyl and 9-fluorenylmethoxycarbonyloxy (Fmoc) protected Naq followed that reported for methyl-protected Naq and began with the alkylation of 1,4-dihydroxy-2-naphthoic acid to form propargyl-1,4-dipropargyloxy-2-naphthoate in a good 79 % yield (Scheme 1). Reduction of this ester to the alcohol proceeded in a 90 % yield with lithium aluminum hydride, and the arylbromide (**1**) was generated with phosphorus tribromide in a high yield of 92 %. This product was used for the asymmetric alkylation of *tert*-butyl *N*-(diphenylmethylene) glycinate to yield backbone-protected propargyl-Naq (**2**) in 84 % yield with a 96.5 % enantiomeric excess (*ee*). Conversion to the free propargyl-Naq amino acid Naq(OProp/OProp) in 91 % yield was effected with ethanedithiol in trifluoroacetic acid. Quantitative backbone protection of the free amino acid with Fmoc-succinimide to Fmoc-Naq(OProp/OProp)-OH (**3**) enabled solid-phase peptide synthetic incorporation of Fmoc-Naq(OProp/OProp)-OH into a helix with an N-terminal cysteine (Figure 1). Native chemical ligation employed standard denaturing conditions at approximately 1 mM of the expressed three-helix thioester fragment with two equivalents of the synthetic peptide in the presence of 200 mM mercaptophenylacetic acid and 50 mM tris(2-carboxyethyl)phosphine.[29] 50–75 % yields after purification improved when the ligation was performed in an anaerobic glovebox, suggesting that slow oxidation of the reaction under ambient conditions may impair ligation efficiency. Prior to activation of Naq, the free cysteine in the semisynthetic bundle was capped with bromoacetamide. Because standard procedures for removing propargyl groups using either strong Lewis acids[27] or palladium-catalyzed reduction[28] led either to hydrolysis of the backbone prior to Naq activation or to very low yields, we used dicobaltoctacarbonyl in TFA to quantitatively activate Naq without side reactions with the diverse unprotected natural amino acids in the maquette.

The spectroscopy and electrochemistry of Naq incorporated into a solvent-exposed helical site matched previous studies exploring the structural and electrochemical coupling of the Naq amino acid in a simple peptide[16,24] (E_{m8} values (midpoint potential at pH 8) of -62 ± 6 mV versus −40 mV; Figure 2), providing a good standard of comparison for electrochemical manipulation in buried Naq designs. The Naq-modified bundle also maintained a helical structure (Figure S3) and the ability to bind the metal–tetrapyrrole cofactors heme and Zn-protoporphyrin IX (ZnPPIX) both separately and together (Figure 3). As observed in previous maquette designs, bis-His ligation of a heme cofactor increases the thermal folding stability, from a melting transition of 40 to 50 °C (Figure S4). In the Naq maquette, one bis-His site has a high affinity for both heme and ZnPPIX; at the lower affinity site, only one of the two available His residues was needed to bind ZnPPIX (Figure 3). It is not clear from design first principles which site has higher affinity and binds one equivalent of heme, leaving the remaining low affinity

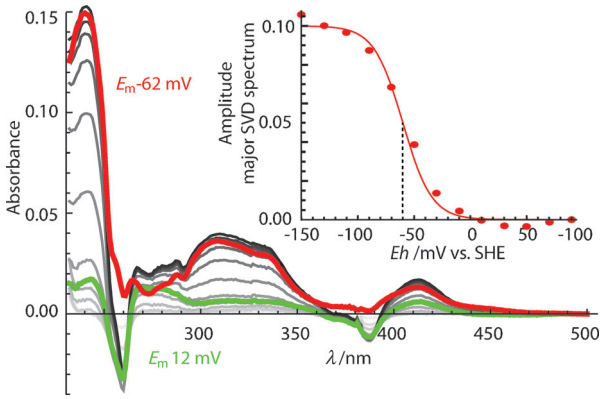

Figure 2. Spectroelectrochemistry of Naq in the maquette shows expected two-electron redox behavior. Singular value decomposition of the full spectral redox titration from +100 mV (light gray) to −150 mV (dark gray) is dominated by two redox sensitive spectral components: the Naq redox spectrum (red; $E_m = -62 \pm 6$ mV, amplitude shown in insert) and the phenazine redox mediator dye (green; $E_m = -7 \pm 7$ mV) added to assure potential measurement accuracy. SHE = standard hydrogen electrode; SVD = singular value decomposition, a function used to delineate spectrum into its components.

site free for subsequent addition of ZnPPIX. However, the symmetric placement of the Naq cofactor between the two sites (Figure 1) maintains similar electron-tunneling distances in either geometry.

Photoexcitation of a bound ZnPPIX in the Naq-containing maquette generates a long-lived triplet excited state that is capable of reducing Naq to its anionic, singly reduced semiquinone form (estimated $E_{m8} = -200$ mV[30]). Charge separation should be detectable by a shortening of the triplet lifetime in the presence of an oxidized Naq cofactor. The formation and decay of the ZnPPIX triplet state after excitation with a $\lambda = 550$ nm laser pulse was observed with transient absorption spectroscopy from 100 ns to 0.1 s (Figure 4). When Naq was prereduced with ammonia borane, and hence not capable of ZnPPIX photoreduction, the triplet decay follows single-exponential kinetics with a millisecond lifetime ($5 \pm 1 \times 10^2$ s^{-1}) similar to that seen in other maquette designs.[15] In the presence of oxidized Naq, the triplet decay is indeed significantly faster and better fit by a stretched exponential $\exp[-(kt)^{\beta}]$, with a rate (k) of $7 \pm 2 \times 10^3$ s^{-1} and a β value, describing the extent of stretching, of 0.3 ± 0.1. Oxidized Naq has a photoprotective effect on the ZnPPIX, presumably because an electron-transfer-shortened lifetime of the excited triplet state provides less opportunity for photobleaching. In contrast, when Naq is reduced, we observe a small progressive loss (approximately 10%) of the ZnPPIX pigment with prolonged laser exposure that tends to lower the triplet amplitude. Points falling below the fit line in Figure 4 were taken after longer laser exposure.

Using our intraprotein electron-tunneling expressions,[18,19] the acceleration of the ZnPPIX triplet state decay is fully attributable to a two-step, forward and back, electron-transfer event. In the process, the photoexcited ZnPPIX reduces Naq to its anionic semiquinone (0.58 eV mean driving force) with a mean cofactor separation of 16 Å and a reasonable reorganization energy for a water exposed cofactor of

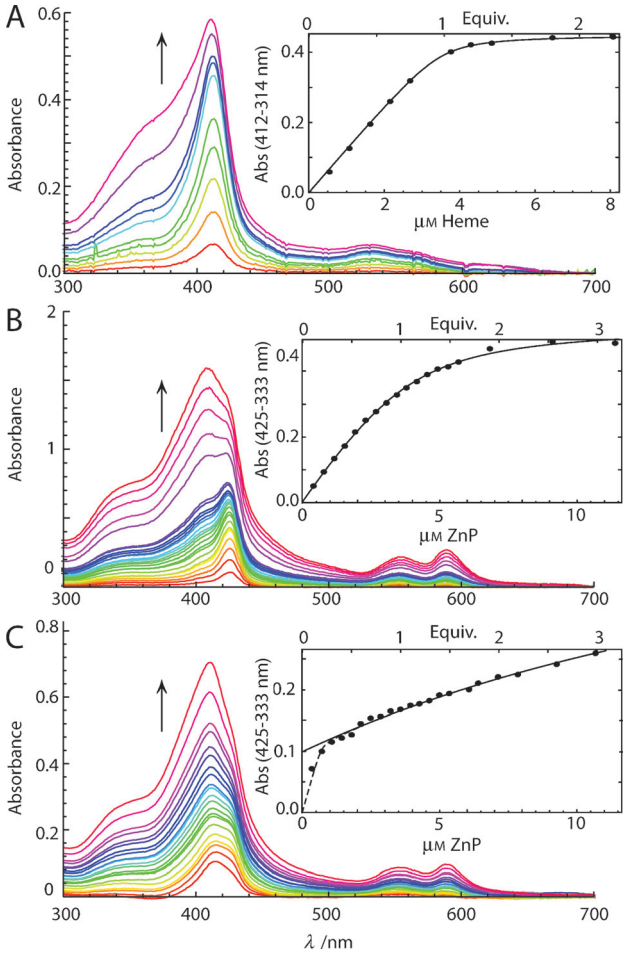

Figure 3. Tetrapyrrole binding titrations with the Naq maquette (see the Supporting Information for complete details). Each panel (A–C) shows increasing absorbance as tetrapyrrole is added with a corresponding inset spectrum monitoring the amplitude at the wavelengths isosbestic for unbound tetrapyrrole: $\lambda = 412$–314 nm for heme addition and 425–333 nm for ZnPPIX addition. A) Heme titration fits to a single K_d value of 70 ± 20 nM. B) ZnPPIX titration fits to a single K_d value of 0.71 ± 0.07 μM. C) ZnPPIX titration to 3.5 μM maquette prebound with 1.1 equivalents heme shows a second-site K_d value of 20 ± 7 μM. The dashed line in (c) reflects residual binding to high affinity site.

circa 1.5 eV,[22,31] followed by a subsequent, fourfold-faster charge recombination. Importantly, this calculated distance matches our initial structural modeling of the maquette.

As in natural proteins, maquette electron-tunneling rates can be modulated by a static or dynamic distribution of edge-to-edge distances, driving forces, or reorganization energies. The complex transient absorption kinetics observed with oxidized Naq can be accounted for by a range of edge-to-edge distances of up to ±1.7 Å, with variance also possible in the reorganization energy and driving force. Residual conformational mobility of the Naq cofactor should be minimized in future designs that bury Naq in the more structured interior where the protein design factors that modulate quinone redox properties and reorganization energies can be systematically explored. The circa −260 mV midpoint potential heme cofactor used here is not effectively reduced by the circa −200 mV Naq semiquinone in a photochemical triad elec-

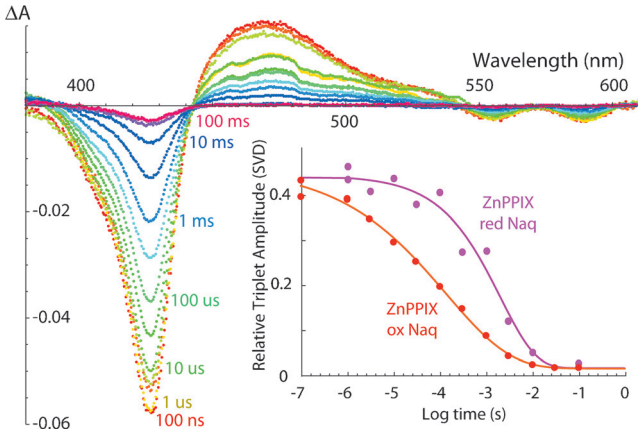

Figure 4. Transient absorption spectroscopy of ZnPPIX-bound Naq-containing bundle. Electron-transfer-active oxidized Naq shortens the lifetime of the excited ZnPPIX triplet state. Singular value decomposition of the full spectral kinetics is dominated by a single spectral component corresponding to the bleach of the ground state ZnPPIX and the absorbance of the ZnPPIX* triplet. Inset: kinetics of this component fit by a simple exponential (purple) or a stretched exponential (red).

tron-transfer relay; planned work with iron tetrapyrroles exhibiting more positive midpoint potentials is needed for a substantially longer-lived charge-separated state.

We have demonstrated incorporation of the naphthoquinone amino acid, Naq, in a semisynthetic four-helix-bundle maquette that binds metal tetrapyrrole cofactors. Within this context, Naq maintains predictable aqueous electrochemistry, allowing use in demonstrating charge separation between a light-activatable zinc porphyrin and the well-positioned quinone. In doing so, we have recapitulated one of the earliest steps of photosynthesis in a completely designed protein system adaptable for systematic protein control of quinone electrochemistry and electron-transfer kinetics.

Acknowledgements

The authors acknowledge Dr. Tammer Farid, Dr. Goutham Kodali, and Dr. Ross Anderson (University of Bristol, UK) for helpful discussions. This research was supported in part by a European Research Council grant (ERC 340451) that funded molecular biology and the US NIH, General Medical Institutes (RO1GM 41048) that funded biophysical characterization of the designed proteins. The US DOE, Office of Basic Energy Sciences, Energy Frontier Research Center (PARC) (DE-SC 0001035) funded the synthesis and characterization of the synthetic naphthoquinone and its assembly in the protein with a photoactive Zn tetrapyrrole.

Keywords: amino acids · electron transfer · photosynthesis · protein engineering · quinones

How to cite: *Angew. Chem. Int. Ed.* **2015**, *54*, 13626–13629
Angew. Chem. **2015**, *127*, 13830–13833

Received: July 30, 2015
Published online: September 14, 2015

[1] D. Schwarzer, P. A. Cole, *Curr. Opin. Chem. Biol.* **2005**, *9*, 561–569.
[2] P. Siman, A. Brik, *Org. Biomol. Chem.* **2012**, *10*, 5684–5697.
[3] P. M. Levine, T. W. Craven, R. Bonneau, K. Kirshenbaum, *Org. Lett.* **2014**, *16*, 512–515.
[4] Y. Zhang, C. Xu, H. Y. Lam, C. L. Lee, X. Li, *Proc. Natl. Acad. Sci. USA* **2013**, *110*, 6657–6662.
[5] M. Chang, C. S. Yee, D. G. Nocera, J. Stubbe, *J. Am. Chem. Soc.* **2004**, *126*, 16702–16703.
[6] Z. Guo, N. W. Woodbury, J. Pan, S. Lin, *Biophys. J.* **2012**, *103*, 1979–1988.
[7] Y. Song, J. Mao, M. R. Gunner, *Biochemistry* **2006**, *45*, 7949–7958.
[8] T. L. Olson, J. C. Williams, J. P. Allen, *Biochim. Biophys. Acta Bioenerg.* **2013**, *1827*, 914–922.
[9] M. R. Gunner, J. Madeo, Z. Zhu, *J. Bioenerg. Biomembr.* **2008**, *40*, 509–519.
[10] M. R. Gunner, P. L. Dutton, *J. Am. Chem. Soc.* **1989**, *111*, 3400–3412.
[11] A. Osyczka, H. Zhang, C. Mathé, C. C. Moser, P. R. Rich, P. L. Dutton, *Biochemistry* **2006**, *45*, 10492–10503.
[12] I. Rudik, C. Thorpe, *Arch. Biochem. Biophys.* **2001**, *392*, 341–348.
[13] S. Ghisla, V. Massey, *Biochem. J.* **1986**, *239*, 1–12.
[14] D. E. Robertson, R. S. Farid, C. C. Moser, J. L. Urbauer, S. E. Mulholland, R. Pidikiti, J. D. Lear, A. J. Wand, W. F. Degrado, P. L. Dutton, *Nature* **1994**, *368*, 425–431.
[15] T. A. Farid, G. Kodali, L. A. Solomon, B. R. Lichtenstein, M. M. Sheehan, B. A. Fry, C. Bialas, N. M. Ennist, J. A. Siedlecki, Z. Zhao, M. A. Stetz, K. G. Valentine, J. L. R. Anderson, A. J. Wand, B. M. Discher, C. C. Moser, P. L. Dutton, *Nat. Chem. Biol.* **2013**, *9*, 826–833.
[16] B. R. Lichtenstein, V. R. Moorman, J. F. Cerda, A. J. Wand, P. L. Dutton, *Chem. Commun.* **2012**, *48*, 1997–1999.
[17] B. R. Gibney, S. E. Mulholland, F. Rabanal, P. L. Dutton, *Proc. Natl. Acad. Sci. USA* **1996**, *93*, 15041–15046.
[18] C. C. Moser, J. M. Keske, K. Warncke, R. S. Farid, P. L. Dutton, *Nature* **1992**, *355*, 796–802.
[19] C. C. Page, C. C. Moser, X. Chen, P. L. Dutton, *Nature* **1999**, *402*, 47–52.
[20] W.-W. Li, J. Heinze, W. Haehnel, *J. Am. Chem. Soc.* **2005**, *127*, 6140–6141.
[21] W.-W. Li, P. Hellwig, M. Ritter, W. Haehnel, *Chem. Eur. J.* **2006**, *12*, 7236–7245.
[22] S. Hay, B. B. Wallace, T. A. Smith, K. P. Ghiggino, T. Wydrzynski, *Proc. Natl. Acad. Sci. USA* **2004**, *101*, 17675–17680.
[23] S. Hay, K. Westerlund, C. Tommos, *J. Phys. Chem. B* **2007**, *111*, 3488–3495.
[24] B. R. Lichtenstein, J. F. Cerda, R. L. Koder, P. L. Dutton, *Chem. Commun.* **2009**, 168–170.
[25] L. Regan, W. F. Degrado, *Science* **1988**, *241*, 976–978.
[26] D. Crich, P. Jayalath, *Org. Lett.* **2005**, *7*, 2277–2280.
[27] S. Punna, S. Meunier, M. G. Finn, *Org. Lett.* **2004**, *6*, 2777–2779.
[28] M. Pal, K. Parasuraman, K. R. Yeleswarapu, *Org. Lett.* **2003**, *5*, 349–352.
[29] E. Johnson, S. Kent, *J. Am. Chem. Soc.* **2006**, *128*, 6640–6646.
[30] A. J. Swallow, *Function of Quinones in Energy Conserving Systems*, Elsevier, Dordrecht, **1982**, pp. 59–72.
[31] K. A. Sharp, *Biophys. J.* **1998**, *74*, 1241–1250.